Mechanism of Helix Induction by Trifluoroethanol: A Framework for Extrapolating the Helix-Forming Properties of Peptides from Trifluoroethanol/Water Mixtures Back to Water[†]

Peizhi Luo and Robert L. Baldwin*

Department of Biochemistry, Beckman Center, Stanford Medical School, Stanford, California 94305-5307

Received March 27, 1997[⊗]

ABSTRACT: To establish a framework for extrapolating the helix-forming properties of peptides from TFE/H_2O mixtures (TFE = 2,2,2-trifluoroethanol) back to water, the thermal unfolding curves have been measured by circular dichroism for four repeating-sequence peptides, with chain lengths from 7 to 22 residues. The unfolding curves were measured between 0 and 50 volume percent TFE and were fitted to the modified Lifson−Roig theory. A single set of helix−coil parameters fits the results for the four peptides at each TFE concentration; only two of the basic helix−coil parameters, $<w>$, the mean helix propagation parameter of residues in the sequence repeat, and ΔH, the enthalpy change per residue on unfolding the helix, are allowed to vary with TFE molarity. The success in fitting these curves over a wide range of experimental variables shows that helix formation is basically the same in TFE/H_2O mixtures as in water. Moreover, a simple model based on a linear dependence of ln $<w>$ and ΔH on TFE molarity can be used to extrapolate the results from 25% TFE (approximately 4 M) back to water. The results also give curves of helix formation induced by TFE at constant temperature, and the properties of these helix induction curves explain some of the puzzling results shown by other peptides in the literature. The average helix propensity increases regularly from 0 to 25% TFE but levels off at higher TFE concentrations, which explains why the extent of helix formation levels off in this range. The change in the apparent cooperativity of thermal unfolding curves in concentrated TFE solutions results from the decrease of the enthalpy change for helix unfolding at higher TFE concentrations. The rapid decrease in the plateau values of apparent helix content with increasing temperature results mainly from the strong temperature dependence of the ellipticity of the complete helix. To determine whether the helix-stabilizing effect of TFE arises from strengthening the hydrogen bonds in the helix backbone, the strength of the hydrogen bond in a model compound, salicylic acid, has been measured in TFE/H_2O mixtures from the pK_a difference between salicylic acid and a similar compound which cannot form the hydrogen bond. The curve of hydrogen bond strength versus increasing TFE concentration matches both in shape and magnitude the increase in average helix propensity in TFE/H_2O mixtures.

TFE/H_2O mixtures are used widely to stabilize peptide helices, following the introduction of TFE[1] by Goodman & Listowsky (1962). Peptides with sequences derived from proteins typically show little or no helix formation in water (Muñoz & Serrano, 1994) but can be induced to form helices in TFE/H_2O mixtures (Filippi et al., 1978; Nelson & Kallenbach, 1986; Segawa et al., 1991; Sönnichsen et al., 1992; Storrs et al., 1992; Jasanoff & Fersht, 1994; Hamada et al., 1995; Cammers-Goodwin et al., 1996; and references therein). The curve of induced helix formation versus TFE concentration is referred to here as the helix induction curve. In principle, it is possible to evaluate the intrinsic helix-forming properties of a peptide in water, when these are too low to be measured directly, by measuring them in TFE/H_2O mixtures (Segawa et al., 1991; Behrends et al., 1997); but it is necessary then to extrapolate the data back to water, and a satisfactory extrapolation procedure has not yet been reported. Accomplishing this task should help to provide quantitative insight into the relation between secondary structure formation and the initiation of protein folding (Dyson & Wright, 1993; Waltho et al., 1993; Shin et al., 1993a,b).

The mechanism by which TFE stabilizes peptides helices is unknown, although two possible mechanisms have been discussed: helix stabilization by direct binding of TFE (Jasanoff & Fersht, 1994) and an indirect mechanism in which the peptide H-bonds in the helix are stabilized by weakening the H-bonding of H_2O to peptide CO and NH groups in the coil form (see Cammers-Goodwin et al., 1996 and references within). Not only peptide helices, but also β-hairpins (Blanco et al., 1994; Ramírez-Alvarado et al., 1996) and even molten globule-like folding intermediates (Buck et al., 1993; Alexandrescu, et al., 1994) can be stabilized by TFE. Thus, it is of general interest to determine the mechanism by which TFE stabilizes helices.

A problem in using helix induction curves measured in TFE/H_2O mixtures to deduce the helix-forming properties of peptides in water is that some characteristics of these curves are not understood: see Nelson & Kallenbach (1986)

[†] This work was supported by NIH Grant GM 31475. P. Luo is a fellow of the Arthritis Foundation. The Mass Spectrometry Facility, University of California, San Francisco, is supported by NIH Grant RR 01614.

* To whom correspondence should be addressed.

[⊗] Abstract published in *Advance ACS Abstracts,* July 1, 1997.

[1] Abbreviations: TFE, 2,2,2-trifluoroethanol; ΔH, enthalpy change for helix formation per mole of residue; CD, circular dichroism; H-bond, hydrogen bond.

S0006-2960(97)00713-7 CCC: $14.00

and Jasanoff & Fersht (1994). (1) It is not clear why helix induction occurs only from 0 to ~40% TFE and, at higher TFE concentrations, reaches a plateau level that is often less than 100% helix. (2) Peptides which show good helix formation in water typically reach plateau levels that apparently are near 100% helix as TFE is added. Although such plateau values are also reached at higher temperatures, the CD plateau values decrease rapidly with increasing temperature. This behavior is unexpected if the plateau values really correspond to almost 100% helix. (3) The apparent cooperativity of helix unfolding appears to be low in TFE/H_2O mixtures although these unfolding curves induced by urea, GdmCl, or heating in water are S-shaped.

Jasanoff & Fersht (1994) made a study of the helix induction curves of four peptides with different sequences in TFE/H_2O mixtures at various temperatures. They noted some of the same phenomena we report here, but they analyzed their results by the two-state model and consequently were unable to determine the helix propensities defined by the Zimm−Bragg (1959) and/or Lifson−Roig (1961) theories. Helix−coil theory is required to analyze the helix−coil transitions even of short peptides (see, for example, Chakrabartty et al., 1991). A basic test of the applicability of helix−coil theory is that, for peptides of varying chain lengths, the helix propensities should be independent of length in repeating-sequence peptides. This requirement is satisfied in the work reported here.

The rationale for our procedure is as follows. We study repeating-sequence peptides to find out if the helix−coil parameters are independent of sequence length. This test has been made in earlier work (Zimm et al., 1959; Scholtz et al., 1990a; Rohl et al., 1992). It has been also used successfully to analyze the denaturant-induced unfolding of peptide helices by urea (Scholtz et al., 1995) and by GdmCl (Smith & Scholtz, 1996). We can make the same test sensitive in the TFE-induced helix with high helical content, if the helix−coil theory is fitted to the thermal unfolding curves in TFE/H_2O mixtures over a wide range of helical populations. The four peptides studied here have the common formula Ac-$(AAKAA)_n$GY-NH_2 ($n = 1-4$) and they have chain lengths varying from 7 to 22 residues.

The thermal helix−coil transitions of the peptides were measured over a wide range of TFE concentrations, 0 to 50 vol %, and were fitted to the modified Lifson−Roig theory (Doig et al., 1994; Rohl et al., 1996) which includes N-capping. Then we used the results to analyze the properties of helix induction curves at constant temperature in TFE/H_2O mixtures. The results show that the helix propensity, or helix propagation parameter, becomes stronger in TFE/H_2O mixtures, but that it reaches a plateau value above 25% TFE.

To investigate whether this helix-stabilizing effect can be explained by strengthening the peptide H-bonds in the helix, we measured the strength of the hydrogen bond in a standard model compound, salicylic acid, in various TFE/H_2O mixtures, to find out if the H-bond becomes stronger when TFE is added. Salicylic acid (*o*-hydroxybenzoic acid) forms a H-bond between the ortho OH and COOH groups, and the strength of the H-bond can be computed from the difference between the COOH pK_a values of *o*-hydroxy- and *p*-hydroxybenzoic acid, since the para compound does not form the H-bond (see Hermans et al., 1963; Shan et al., 1996). The data for the change in H-bond strength with TFE concentration are compared to the change in mean helix propensity of the five-residue repeat (AAKAA) in the peptides studied here.

MATERIALS AND METHODS

Peptides and Model Compounds. Peptides were synthesized by the solid phase method using fluorenylmethoxycarbonyl (Fmoc) chemistry. Pentafluorophenyl esters of Fmoc-protected amino acids were used for all coupling reactions except for Ala, where the free acid of Fmoc-Ala and in situ activation reagent TBTU were used. The crude peptides were purified by preparative C18 reverse phase column, and the purity of the peptide was confirmed to be >95% by analytical C18 reverse phase column chromatography using the Pharmacia FPLC system. The peptide identity was confirmed by FAB mass spectrometry. The salicylic acid and *p*-hydroxybenzoic acid were from Aldrich in the highest purity available. The 99+% 2,2,2-trifluoroethanol (TFE) was purchased from Aldrich.

Preparation of Peptide Samples for CD Measurements. The peptide stock solutions of ~1 mM were prepared, and their concentrations were determined by measuring tyrosine absorbance in 6 M guanidine hydrochloride solutions at pH 6.5 using $\epsilon_{275} = 1450\ M^{-1}\ cm^{-1}$ (Brandts & Kaplan, 1973). CD samples were prepared by adding aliquots of a peptide stock solution into 2 mL of 0−50% TFE (TFE volume added/total volume added), containing 20 to 50 μM peptide, 100 mM NaCl, and 1 mM each of sodium borate, sodium citrate, and sodium phosphate at pH 7.0. CD spectra and thermal melting curves were taken on an Aviv 60DS spectropolarimeter equipped with a Peltier temperature control unit. Ellipticity of peptides was measured at 222 nm and is reported as mean residue ellipticity in units of deg $cm^2\ dmol^{-1}$. The thermal transition data were recorded every 2 or 5 °C in heating but every 10 °C in cooling; the sample was equilibrated for ca. 6 min at each temperature to achieve complete reversibility.

Determination of pK_a and pH Measurements. The pH measurements were made on a Orion research digital ionalyzer pH meter equipped with a combined glass electrode. The pH meter and electrode were calibrated using standard pH buffers at four points: 2.00, 4.00, 7.00, and 10.00 in aqueous solution at 25 °C. The pH electrode was immersed in a given buffer and/or solvent, and the pH reading was stable over several days before measurements. The pH reading is accurate to ±0.01 from pH 2.00 to 7.00 but could be off by ±0.03 around pH 10.00. Most pH values were measured in the range 2 to 7 with excellent linear response. The apparent meter reading was reported with no correction for the effects of salt concentration and solvent composition. Although these effects will influence the apparent pK_a values determined at different TFE concentrations, they will have little effect on the difference between pK_a values of the COOH group in *o*-hydroxy- and *p*-hydroxybenzoic acids at an identical TFE concentration (Bates et al., 1963), from which the H-bond strength of salicylic acid is computed.

The pK_a values were determined from fitting the pH titration curves of *o*-hydroxy- and *p*-hydroxybenzoic acids in 100 mM NaCl in TFE/H_2O mixtures. The UV difference spectra of *o*-hydroxy- and *p*-hydroxybenzoic acids in TFE solutions were measured at 241 and 261 nm, respectively,

with a UVIKON UV/vis spectrophotometer. To ensure that the sample concentration and the solvent composition of TFE/H_2O mixtures remain unchanged during pH titration, two identical samples were prepared: one for measuring the pH titration curve, and a "dummy" sample for storing the pH electrode whenever it is removed from the cuvette in order to measure the absorbance. The temperature was controlled at 25 °C. To prevent esterification of the acids with TFE, which occurs slowly, TFE was pipetted into the sample immediately before beginning the titration. After adding concentrated HCl or NaOH solution to the cuvette, a pH electrode was inserted into the cuvette and the pH was read. Then the pH electrode was taken out and stored in the dummy sample while the absorbance of the titrated sample was read. Good reproducibility of the spectral titration curve was observed if this procedure was followed.

Data Analysis. Nonlinear least squares analysis was used to fit the thermal unfolding curves to modified Lifson−Roig helix−coil theory (Doig et al., 1994; Rohl et al., 1996), with the following assumptions. First, the helical content of a peptide is proportional to its mean residue ellipticity measured by CD at 222 nm. Second, the equation for calculating 100% helix is given by

$$\Theta_H = (\Theta_H(0) + (\partial\Theta_H/\partial T)T)(1 - x/\mathrm{Nr}) \qquad (1)$$

where Θ_H is in units of deg cm^2 dmol^{-1}, T is in °C, $x = 3$ is the number of non-H-bonded peptide CO groups in a carboxyamidated peptide, and Nr is the number of residues in a peptide chain.

The values of $\Theta_H(0)$ at 0 °C and its temperature dependence, $\partial\Theta_H/\partial T$, for an infinite helix, are taken to be −44000 and 250, respectively. The length correction $(1 - x/\mathrm{Nr})$ is applied to $\Theta_H(0)$ as well as to $\partial\Theta_H/\partial T$, as shown in eq 1. These values of Θ_H and $\partial\Theta_H/\partial T$ are larger than the values used earlier (Scholtz et al., 1991a). The reason is given in Discussion. More data, taken over a wide range of experimental variables, are needed to verify or revise these fundamental parameters in the helix−coil theory. The values of Θ_C as a function of temperature are taken from the measured values for the 7-mer; Θ_C is observed to be a linear function of temperature at each TFE concentration (Figure 2).

Finally, the fraction helix, f_H, of a peptide is defined as ratio of the average number of helical H-bonds divided by the total number of H-bonds available in a peptide with Nr residues.

$$f_H = \langle n_H \rangle/(\mathrm{Nr\text{-}2}) \qquad (2)$$

The predicted fraction helix is calculated from the modified Lifson−Roig helix−coil model as a function of the peptide chain length and of the helix parameters (w, v, n, and c) of each residue.

The measured value of f_H is obtained from the mean residue ellipticity of each peptide according to the following equation.

$$f_H = (\Theta_{obs} - \Theta_C)/(\Theta_H - \Theta_C) \qquad (3)$$

The NONLIN software package was used for nonlinear least-squares fitting with the error reported at 67% confidence level (Johnson et al., 1981)

Determination of pK_a. The apparent pK_a is determined by fitting UV difference absorbance of model compounds at different pH values to the following equation. The nonlinear least-squares procedure of Kaleidagraph is used, with the standard error reported at 67% confidence level.

$$\mathrm{p}K_a = \mathrm{pH} - \log([B^-]/[HB]) \qquad (4a)$$

$$A_{obs} = (A_{min} - A_{max})\, 10^{(\mathrm{pH}-\mathrm{p}K_a)}/(10^{(\mathrm{pH}-\mathrm{p}K_a)} + 1) + A_{max} \qquad (4b)$$

where A_{obs} is the absorbance of a model compound at different pH values relative to the same sample at a fixed pH. A_{min} and A_{max} are the UV absorbance values in the conjugate base form (high pH) and in the acid form (low pH), respectively.

RESULTS

Properties of Thermal Transition Curves in TFE/H_2O Mixtures and the Procedure for Fitting Them. The thermal transition curves of the four peptides, measured at four TFE concentrations (0, 10, 20, and 35%) are shown in Figure 1. Although peptide AK7 exhibits the CD spectra typical of the coiled conformations, and therefore is not expected to show any measurable helix formation, its value of $[\Theta]_{222}$ does change significantly with temperature and TFE concentration. Measurements on the 7-mer are given in Figure 2. The apparent cooperativity of the thermal transition curves decreases with increasing TFE concentration, and the S-shaped unfolding curve of the 22-mer at 0% TFE becomes almost linear at 35% TFE. Nevertheless, when the curves are fitted to helix−coil theory (the modified Lifson−Roig theory of Doig et al., 1994, revised by Rohl et al., 1996), by fixing the helix nucleation constant at its value in water and allowing the helix propagation parameter w to vary both with TFE concentration and temperature, the transition curves can be fitted satisfactorily. The solid lines in Figure 1 show the fitted curves. The other parameters are fixed at their values in water (see Methods), except for the dependence of Θ_c (the mean residue ellipticity of the coil form) on temperature, which was measured for the 7-mer (Figure 2) and was found to depend significantly on TFE concentration. Details of the fitting procedure are given below. The helix propensities of the five residues (AAKAA) in the sequence repeat were averaged to give the mean propensity $\langle w \rangle$ and the dependence of $\ln\langle w \rangle$ on TFE concentration and temperature was measured (Figure 3).

In experiments of this kind, using repeating-sequence peptides to explore the dependence of helix−coil parameters on certain variables, it is standard practice to use the homopolymer approximation, in which the helix propensities of the different residues are averaged and the peptide is replaced by an equivalent homopolymer with an average $\langle w \rangle$ (Scholtz et al., 1991a; Rohl et al., 1992). Here we use a partial homopolymer approximation in which averaging is applied only to the AK residues in the sequence repeat, since the C-terminal Gly and Tyr residues have very different helix propensities from A and K (Rohl et al., 1996), and Gly, which separates Tyr from the rest of the helices (Chakrabartty et al., 1993), still remains as a strong helix breaker at 40% TFE (Rohl et al., 1996). Because w is an

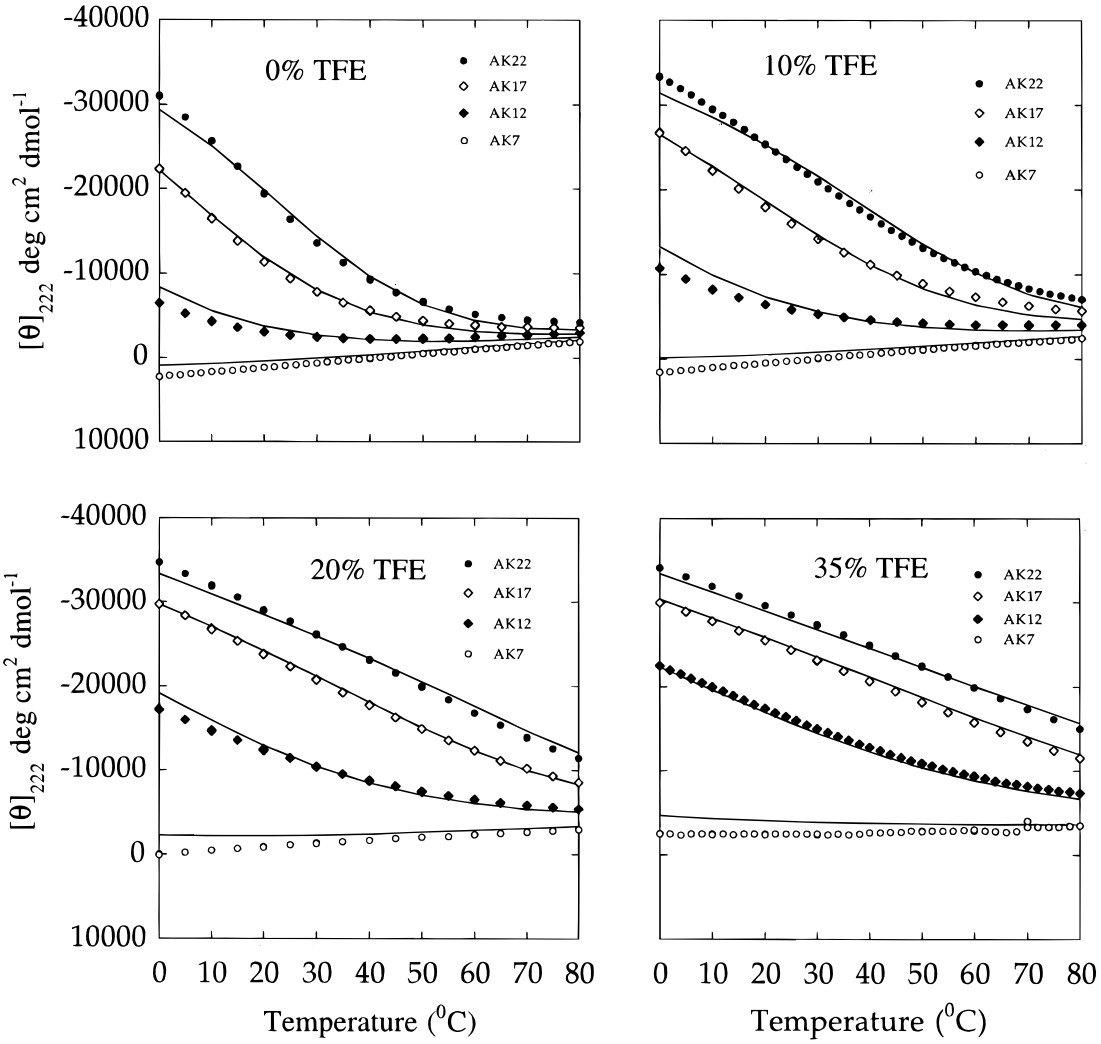

FIGURE 1: Thermal transition curves for four peptides with the sequence Ac-(AAKAA)$_n$-GY-NH$_2$, containing 7 (AK7), 12 (AK12), 17 (AK17), and 22 (AK22) residues. The curves are measured at 0, 10, 20, and 35% TFE (0.1 M NaCl, 1 mM each of sodium phosphate, sodium borate, and sodium citrate, pH* 7.0). The fitted curves are generated by the modified Lifson−Roig theory (Doig et al., 1994; Rohl et al., 1996), using (−44000 + 250*T*) * (1 − 3/Nr) for 100% helix, and taking the base line of the coil form as well as the corresponding Δ*H* values from Figures 2 and 3b, respectively.

equilibrium constant, ln <*w*> is allowed to vary with temperature according to the van't Hoff relation

$$\ln\langle w\rangle = \ln\langle w_0\rangle - (\Delta H/R)(1/T - 1/T_0) \qquad (5)$$

where <w_0> is the value of <*w*> at the reference temperature T_0 and Δ*H* is the enthalpy change per residue upon helix formation. Studies of urea-induced and GdmCl-induced unfolding of peptide helices (Scholtz et al., 1995; Smith & Scholtz, 1996) have shown that ln <*w*> is a linear function of cosolvent molarity, as expected from studies of using the linear extrapolation model to represent protein unfolding, and we try using the same linear dependence on TFE molarity (C) here (Figure 3A),

$$\ln\langle w\rangle = \ln\langle w_0\rangle - (m/RT)C \qquad (6)$$

Variation of Helix−Coil Parameters with TFE Molarity. The values of ln<*w*> fit the linear extrapolation model up to about 4 M TFE (about 25% TFE). As a last step in fitting the results (see Methods), a global fit of all thermal helix−coil transition curves was made, including data from 0−50% TFE, and Δ*H* and Θ_H (the value of $[\Theta]_{222}$ for an infinite helix at 0 °C) were allowed to float. The results (Figure 3, parts b and c) indicate that Δ*H* decreases strongly with TFE molarity and the decrease is linear within error, while Θ_H is independent of *C* within error. Thus, the decrease in the apparent cooperativity of the thermal transition curves at high TFE concentrations (Figure 1) presumably results from a strong dependence of Δ*H* on TFE concentration.

Data from the thermal helix−coil transition curves are used to give TFE helix induction curves at four different temperatures in Figure 4. The solid lines are given by the helix−coil parameters from the global fit of the thermal transition curves. The lines fit the experimental points satisfactorily except for overprediction of the helix content of the 12-mer at 0 °C and underprediction of the helix content of the 22-mer at 0 °C. The same effect has been observed in a study comparing the helix contents of these peptides measured by circular dichroism and by hydrogen exchange (C. A. Rohl, 1996). The TFE helix induction curves in Figure 4 show clearly one of the puzzling features noted in the earlier studies (Nelson & Kallenbach, 1986; Jasanoff & Fersht, 1994): the plateau values of $[\Theta]_{222}$ and therefore helix content at 40% TFE decrease strongly with increasing temperature for all three peptides.

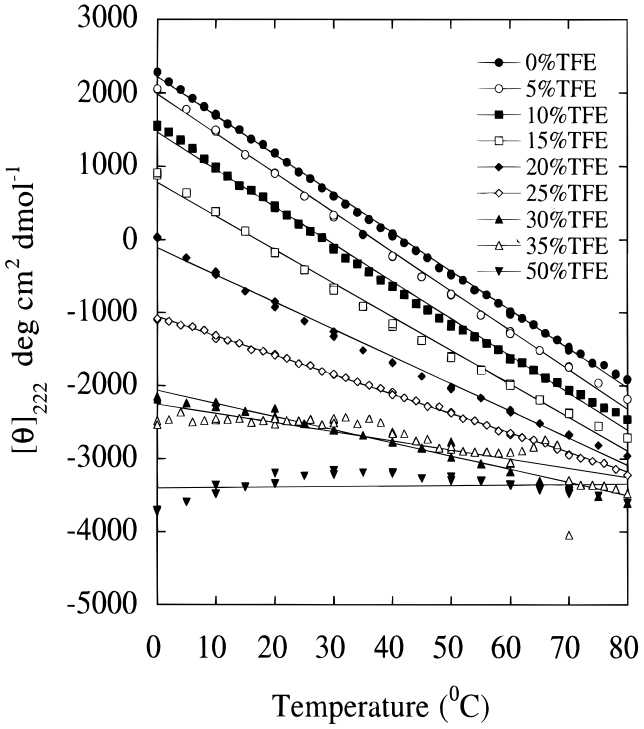

FIGURE 2: The mean residue ellipticity of peptide AK7, $[\Theta]_{222}$, was measured as a function of temperature from 0 to 50% TFE. The temperature dependence at each TFE concentration was fitted to a straight line. The intercept and slope at each TFE concentration were used to provide values for Θ_C at 0 °C and its temperature coefficient $\partial\Theta_C/\partial T$.

H-Bond Strength of Salicylic Acid in TFE/H_2O Mixtures. The rationale for measuring the H-bond strength of salicylic acid from the difference between the pK_a values of the COOH group in *o*-hydroxy and *p*-hydroxybenzoic acids is illustrated in Figure 5a. Salicylic acid is a standard model compound for analyzing the strength of an H-bond in aqueous solution (Hermans et al., 1963; Shan & Herschlag, 1996) because an unusually strong H-bond is formed as the result of closing a six-member ring. The COOH pK_a values can be measured accurately from the change in UV absorbance accompanying ionization. The uncharged form of *o*-hydroxybenzoic acid probably also forms an H-bond, and the pK_a shift gives the increase in H-bond strength caused by forming a charged H-bond versus an uncharged H-bond. The apparent pH measured with a glass electrode in TFE/H_2O mixtures is denoted as pH*, to emphasize that pH* itself does not give the conventional hydrogen ion activity when the glass electrode is used to measure pH in a mixtured solvent (Bates et al., 1963). The assumption is made here that this mixed-solvent problem has little effect on the measurement of the pK_a difference between *o*-hydroxy- and *p*-hydroxybenzoic acids (Bates et al., 1963).

The 25 °C titration curves of *o*-hydroxy- and *p*-hydroxybenzoic acid at 0%, 25%, and 50% TFE are given in Figure 5b. It can be seen that fairly large pK_a shifts are observed in 25% and 50% TFE, and that the pK_a shifts are different for *o*-hydroxy- versus *p*-hydroxybenzoic acid. It is also evident that forming a charged H-bond depresses the pK_a of *o*-hydroxybenzoic acid by more than 1.5 pH units. The results listed in Table 1 are given in Figure 6a as H-bond strength ($\Delta G°$) versus TFE molarity. The strength of the H-bond increases by almost 200 cal between 0 and 4 M TFE

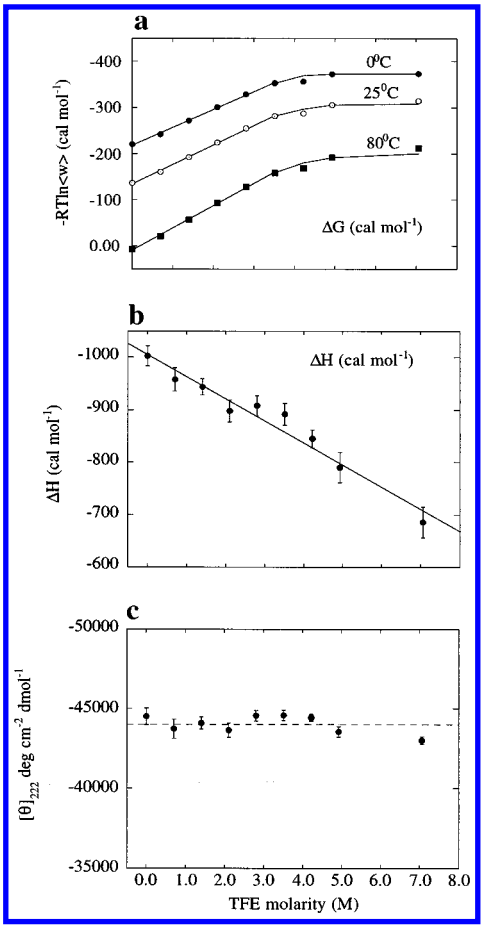

FIGURE 3: (a) $-RT\ln\langle w\rangle$ (the mean value of the helix propagation parameter) versus TFE molarity at 0, 25, and 80 °C. $\langle w\rangle$ values were determined from fitting the thermal transition curves of peptides at each TFE concentration, as shown in Figure 1. $-RT\ln\langle w\rangle$ can be fitted to a linear function of TFE molarity from 0 to 4 M (~25%) TFE at each temperature, but levels off at higher TFE concentration. (b) The enthalpy change per residue upon helix formation, ΔH, as a function of TFE molarity. (c) $[\Theta]_{222}$ of an infinite helix at 0 °C, $\Theta_H(0)$, fluctuates near an average value of −44000 (dashed line).

and then levels off. This behavior is compared with the change in $\Delta G°$ at 25 °C for helix propagation ($\Delta G° = -RT\ln\langle w\rangle$) in Figure 6b. The shapes of the two curves match each other within error.

DISCUSSION

The Helix-Forming Process in TFE/H_2O Mixtures. Our results indicate that the process of helix formation is basically the same in going from H_2O to TFE/H_2O mixtures, even though helix formation is driven by a favorable enthalpy change in water (Figure 3b), and this mode changes to becoming entropy driven at higher TFE concentrations (data not shown) in agreement with earlier results (Conio et al., 1970). The thermal transition curves of three repeating-sequence peptides (12, 17, and 22 residues) can be fitted with a single set of helix−coil parameters in TFE/H_2O mixtures as in water. Only two of the basic helix−coil parameters, $\langle w\rangle$ and ΔH, and one descriptive parameter, Θ_C, need to be made dependent on TFE molarity. A single value of $\langle w\rangle$ reproduces the helix contents of peptides varying in chain length from 12 to 22 residues. The results cannot be fitted by a two-state model (see Jasanoff & Fersht, 1994) if the parameter describing helix propagation is

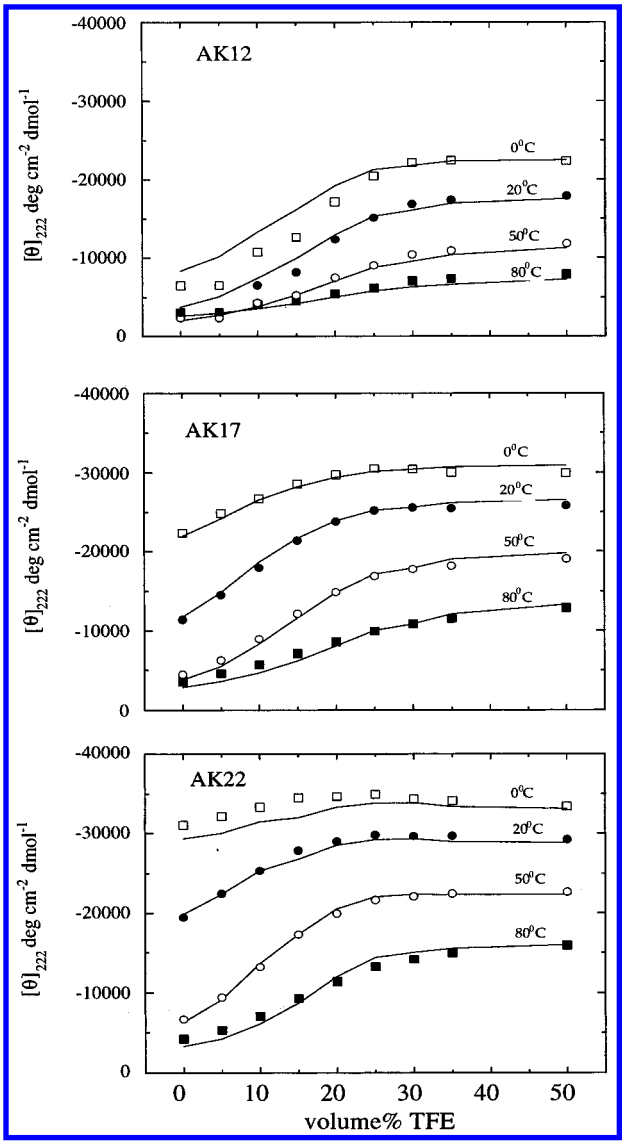

FIGURE 4: The helix induction curves of $[\Theta]_{222}$ versus TFE concentration for peptides AK12, AK17, and AK22 at 0, 20, 50, and 80 °C. The solid lines are transformed from the thermal transition curves (Figure 1) given by the helix−coil parameters as shown in Figure 3.

required to be independent of the length of the repeating sequence.

Some reasons for doubting that such a simple result would be found are given in the introduction. Our results provide plausible explanations for these effects. The helix contents of the peptides level off above 4 M TFE because the rapid increase in helix propensity with TFE concentration levels off above 4 M. In turn, an explanation for this leveling-off effect is provided by finding (see below) that the H-bond strength in a model compound, salicylic acid, increases with TFE concentration but levels off above 4 M. The rapid decrease with increasing temperature in the plateau values of apparent helix content results mainly from the strong temperature dependence of Θ_H. The apparent loss of cooperativity in thermal unfolding at high TFE concentrations probably results from the decrease in ΔH because, for an infinite polypeptide, the slope of the thermal transition curve at its midpoint is inversely proportional to ΔH (Applequist, 1963).

A caveat must be attached to the conclusion that the nature of the helix-forming process remains unchanged in TFE/H_2O mixtures. Helix formation is monitored here by circular dichroism, which gives only the average helix content of a peptide. Deviations from normal helix formation in TFE/H_2O mixtures have apparently been observed (Rohl, 1996) when the process is monitored instead by NMR-hydrogen exchange (Rohl et al., 1992; Rohl & Baldwin, 1994), a method which gives information about the helix contents of individual residues. It is unclear, however, whether these results reflect changes in the process of helix formation or in the validity of the assumptions made to analyze the results.

Table 1. Measurement of the H-Bond Strength of Salicylic Acid from the Difference between the pK_a Values of the COOH Group in *o*-Hydroxy- and *p*-Hydroxybenzoic Acids in TFE/H_2O Mixtures at 25 °C[a]

volume % TFE	pK_a (obs)	pK_a (int)	log K_f
0	2.85 ± 0.01	4.38 ± 0.01	1.53 ± 0.01
5	2.90 ± 0.01	4.46 ± 0.01	1.56 ± 0.01
10	2.94 ± 0.01	4.54 ± 0.02	1.60 ± 0.02
15	3.03 ± 0.02	4.64 ± 0.02	1.61 ± 0.03
20	3.06 ± 0.01	4.72 ± 0.03	1.66 ± 0.03
25	3.22 ± 0.02	4.89 ± 0.01	1.67 ± 0.02
30	3.29 ± 0.04	4.97 ± 0.03	1.68 ± 0.05
40	3.42 ± 0.01	5.10 ± 0.03	1.68 ± 0.03
50	3.53 ± 0.01	5.20 ± 0.02	1.67 ± 0.02

[a] The values of pK_a (obs) and pK_a (int) were determined from fitting pH* titration curves of *o*-hydroxy- and *p*-hydroxybenzoic acids, respectively, measured by UV difference spectra at 241 and 261 nm, respectively, in 100 mM NaCl, at 25 °C. The values of log K_f, corresponding to the H-bond strength of salicylic acid (see Figure 5a), were calculated from log K_f = pK_a (int) − pK_a (obs).

Comments on Values of CD Parameters. Some comments should be made about the values of the parameters used in fitting. Two base lines for 100% helix and 100% coil are needed to convert the ellipticities of α-helical peptides into values of percent helix (eqs 1 and 3). These temperature-dependent CD spectra cannot yet be measured directly. Accurate values of these parameters are needed to determine the helix−coil parameters (Chakrabartty et al., 1994; Muñoz & Serrano, 1994; Rohl et al., 1996). These parameters were fitted originally (Chen et al., 1974) from CD data on proteins with known secondary structures obtained from their X-ray structures. It was realized later that tertiary interactions also contribute significantly to the CD spectra of native proteins. More recently, these parameters were obtained from the thermal transition curves of five peptides with chain lengths varying from 14 to 50 residues, and with the repeating unit of (AEAAKA) flanked by two aromatic groups, Tyr at the N-terminus and Phe at the C-terminus (Scholtz et al., 1991a). The ellipticity of the complete helix depends on chain length because of the unsatisfied amide backbone hydrogen bonds at the peptide termini (Chen et al., 1974; Scholtz et al., 1991a). A revised value of $\Theta_H(0) = -42500$ (Scholtz et al., 1995) changed from the previous −40000 (Scholtz et al., 1991a), was found to fit quite well the urea-induced and GdmHCl-induced unfolding curves of peptide helices at 0 °C. When these peptides were made in 1991 (Scholtz et al., 1991a), it was not yet known that a N- or C-terminal Tyr should be separated from the helix by a Gly residue (this was found by Chakrabartty et al., 1993), to prevent unwanted contributions to the CD spectrum at 222 nm. This effect may account for the difference between the value of $\Theta_H(0)$ found here and found earlier.

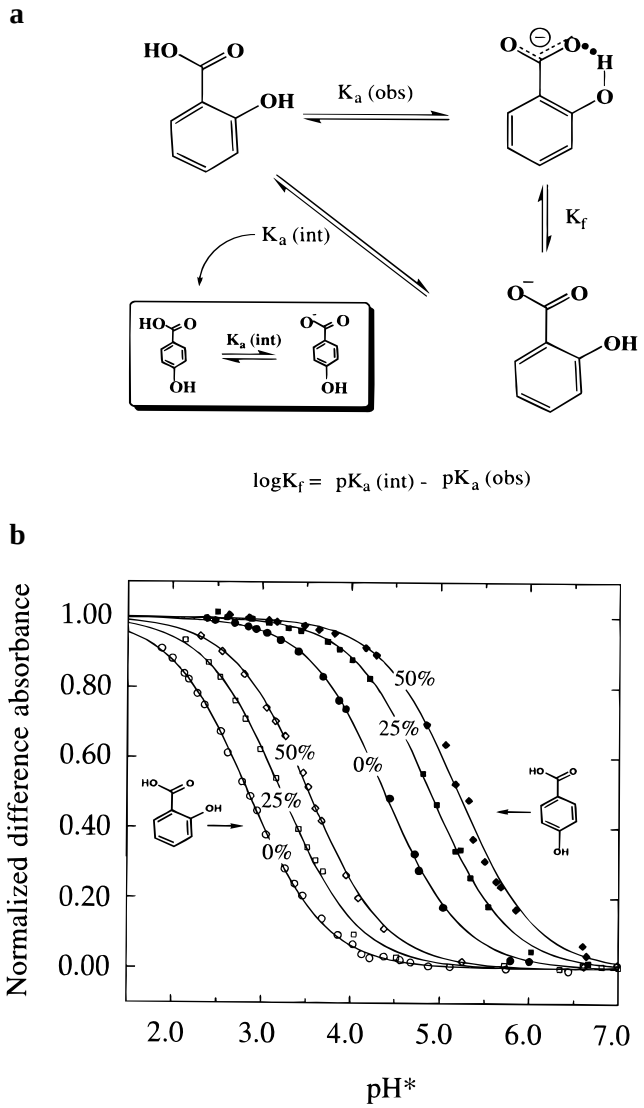

FIGURE 5: (a) Scheme for measuring the hydrogen bond strength of salicylic acid from the difference between the pK_a values of the COOH group in *o*-hydroxy- and *p*-hydroxybenzoic acids. (b) pH* titration curves of *o*-hydroxy- (empty symbol) and *p*-hydroxy- (solid symbol) benzoic acids at 25 °C measured at 241 and 261 nm, respectively. The UV difference absorbance is normalized and plotted against pH* at 0% (circle), 25% (square), and 50% (diamond) TFE solutions.

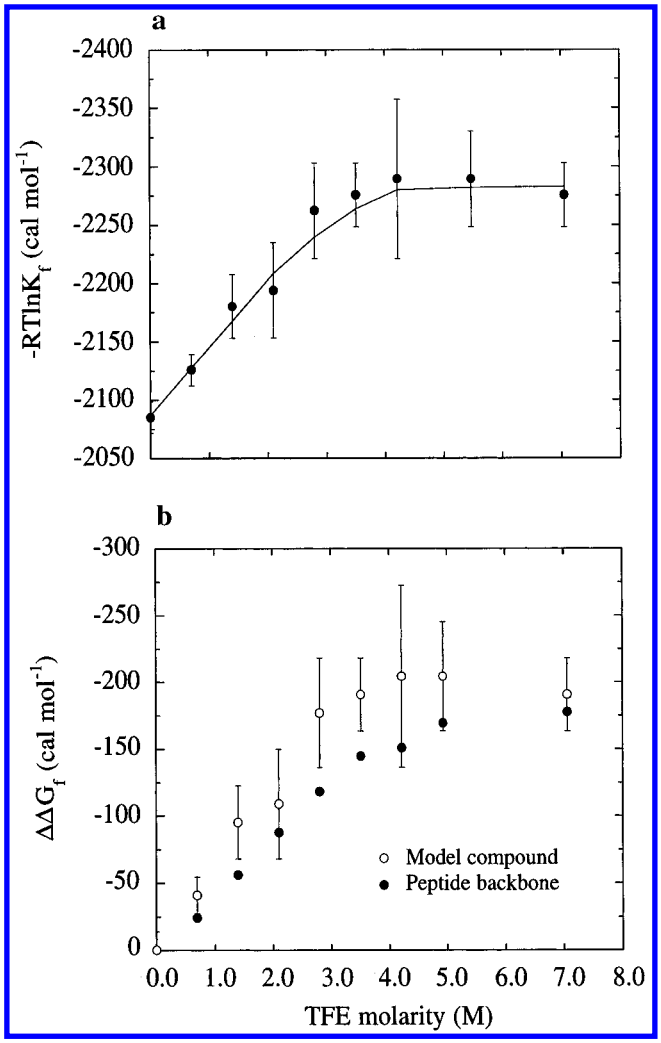

FIGURE 6: (a) The H-bond strength, $\Delta G° = -RT \ln K_f$, at 25 °C, of salicylic acid versus TFE molarity, with the error shown at 67% confidence level. (b) Comparison between the TFE-dependence of the H-bond strength of salicylic acid (Figure 6a) and the corresponding behavior of $\Delta G° = -RT \ln \langle w \rangle$ for helix propagation, at 25 °C, shown in Figure 3a. To show the effect of TFE on the H-bond strength of both systems, the data points in panel b are given relative to their corresponding values in water.

When the temperature dependence of Θ_H, or $\partial\Theta_H/\partial T$, is changed to 250, the fitted curves reproduce much better the apparent cooperativity of the thermal transition curves in TFE/H_2O mixtures (Figures 1 and 4). Therefore, we fixed $\partial\Theta_H/\partial T$ at 250 and found that this value fits satisfactorily the thermal transitions measured earlier (Scholtz et al., 1991a), with Θ_H (0) set at −42500. Once the value of $\partial\Theta_H/\partial T$ is fixed at 250, the fitting procedure becomes straightforward and only $\langle w \rangle$, ΔH, and $\Theta_H(0)$ are allowed to float here. The values for Θ_C and the temperature dependence of Θ_C are taken from measured values for the 7-mer (Figure 2). As a result, Θ_H at 0 °C is found to fluctuate near −44000 across the entire range of TFE concentration (Figure 3c). This value of −44000 for Θ_H is close to −42500 introduced recently (Scholtz et al., 1995; Smith & Scholtz, 1996; Rohl et al., 1996), but is substantially higher than the original value of −40000 (Scholtz et al., 1991a).

Correlation between Helix Propensity and H-Bond Strength. Comparison between the H-bond and helix propensity results shows that the H-bond strengthening effect is large enough to account for the entire increase in helix propensity (Figure 6b). The behavior of the H-bond in salicylic acid in TFE/H_2O mixtures cannot be expected to mimic exactly the behavior of the peptide H-bond. The pK_a difference between *o*- and *p*-hydroxybenzoic acid depends on the difference between the H-bond strength of the charged and uncharged H-bonds in salicylic acid, and charged H-bonds behave differently from uncharged H-bonds in the presence of a less polar solvent such as TFE (Shan & Herschlag, 1996). The peptide H-bond links a CO and NH group, each of which carries a partial charge that is substantial but smaller than a unit formal charge. This difference between charged and uncharged H-bonds may contribute to the slightly but consistently higher H-bond strength in salicylic acid relative to the peptide backbone, as shown in Figure 6b.

Although we have demonstrated here that strengthening the peptide H-bond is the major factor in stabilizing peptide helices in TFE/H_2O mixtures, it is likely that some preferential interaction (see Bixon & Lifson, 1966) also occurs between the helix and TFE relative to H_2O. For example, different sets of amino acids (such as nonpolar versus polar

β-branched residues) undergo characteristically different changes in helix propensity in going from H_2O to 40% TFE (Rohl et al., 1996), although all amino acids studied show increases in helix propensity. These differences are indicative either of side-chain specific preferential interactions of amino acid residues, or of side-chain specific interference with main chain H-bonds.

Dependence of ΔH *on TFE Molarity.* The decrease of ΔH with TFE molarity (Figure 3b) is surprising for the following reason. The mean helix propensity $<w>$ increases with TFE concentration (Figure 3a), and the alanine peptide helix is stabilized in water by the favorable ΔH of forming the helix backbone (Scholtz et al., 1991a,b; Wang & Purisima, 1996). Thus, it is surprising to see $<w>$ increasing and ΔH decreasing with TFE concentration. One reason may be a preferential interaction with TFE relative to H_2O between the helix versus the coil forms of the peptide. Preferential interactions of this kind typically affect ΔH for the helix−coil transition in mixed solvents (Bixon & Lifson, 1966; Lotan et al., 1967). The classic example is poly-γ-benzyl-L-glutamate in mixtures of ethylene dichloride and dichloroacetic acid: the helix actually forms at high temperatures, and the coil form is stable at room temperature (Zimm et al., 1959).

Ben-Naim (1991) and Yang et al. (1992) predict that the ΔH of helix formation should change from being favorable in water to being unfavorable when a helix is buried inside a protein because there are H-bonds between H_2O and the peptide CO groups in a helix exposed to water, and the H-bonded H_2O is stripped off as the helix is buried during folding; this effect is predicted to produce an unfavorable enthalpy change. To find out if this effect is responsible for the decrease in ΔH with TFE concentration, we measured the thermal helix−coil transitions of these peptides in 100% TFE. Our preliminary result is that thermal unfolding still occurs with increasing temperature, indicating that the sign of ΔH remains the same, although there is a further decrease in apparent cooperativity, which suggests that ΔH is quite small, about −0.1 kcal/mol. The value of ΔH in pure TFE deviates from the extrapolated value of −0.4 kcal/mol from Figure 3b. The difference may be caused by the lack of NaCl in 100% TFE, which can affect the helix−coil transition, or the plot may simply become nonlinear above 7 M TFE.

Concluding Comments. The effect of TFE in strengthening peptide H-bonds, found here with peptide helices, can explain why TFE stabilizes β-hairpins and a molten globule-like intermediate called the TFE state (Buck et al., 1993, 1995; Alexandrescu et al., 1994; Fan et al., 1993; Schönbrunner et al., 1996), which has well-populated secondary structure in the absence of extensive tertiary interactions. The major concern over using TFE to probe secondary structures of peptides and proteins is the relevance of the TFE-induced structure to the native conformation. Although TFE is known to promote consistently native-like helical structure in most peptides, it does induce nonnative helical structure in some cases, for example, in the loop and/or β-sheet regions of the native protein structure (Sönnichsen et al., 1992; Fan et al., 1993; Buck et al., 1995). Close examination indicates that the nonnative structure induced by TFE is highly flexible, without stable helical H-bonds (Buck et al., 1995; Schönbrunner et al., 1996). In contrast, stable and native-like H-bonds are clearly identified in TFE-stabilized β-hairpins (Blanco et al., 1994; Ramírez-Alvarado et al., 1996) and native-like β-structure (Schönbrunner et al., 1996), as in α-helices (Buck et al., 1995). The ability of TFE to induce the structure of β-hairpins (Blanco et al., 1994; Ramírez-Alvarado et al., 1996) is striking. The β-hairpin induction curves likewise show a continuous increase in structure formation from 0 to 30% TFE, and then level off at higher TFE concentrations (Ramírez-Alvarado et al., 1996). Our study of the mechanism by which TFE stabilizes helices argues that this puzzling behavior is expected if strengthening H-bonds is the major energetic reason for stabilizing these β-hairpins (Blanco et al., 1994; Ramírez-Alvarado et al., 1996).

ACKNOWLEDGMENT

We thank Dr. Carol Rohl for providing the peptides used here and for helpful discussions, and we also thank Shu-ou Shan and Dr. Hong Qian for their discussion. Mass spectra of the peptides were kindly provided by the Mass Spectrometry Facility of the University of California, San Francisco.

REFERENCES

Alexandrescu, A. T., Ng, Y.-L., & Dobson, C. M. (1994) *J. Mol. Biol. 235*, 587−599.
Applequist, J. (1963) *J. Chem. Phys. 38*, 934−941.
Bates, R., Paabo, M., & Robinson, R. A. (1963) *J. Phys. Chem. 67*, 1833−1838.
Behrends, H. W., Folkers, G., & Beck-Sickinger, A. G. (1997) *Biopolymers 41*, 213−231.
Ben-Naim, A. (1991) *J. Phys. Chem. 95*, 1437−1444.
Bixon, M., & Lifson, S. (1966) *Biopolymers 4*, 815−821.
Blanco, F. J., Jiménez, M. A., Pineda, A., Rico, M., Santoro, J., & Nieto, J. L. (1994) *Biochemistry 33*, 6004−6014.
Brandts, J. R., & Kaplan, K. J. (1973) *Biochemistry 12*, 2011−2024.
Buck, M., Radford, S. E., & Dobson, C. M. (1993) *Biochemistry 32*, 669−678.
Buch, M., Schwalbe, H., & Dobson, C. M. (1995) *Biochemistry 34*, 13219−13232 (1995).
Cammers-Goodwin, A., Allen, T. J., Oslick, S. L., McClure, K. F., Lee, J. H., & Kemp, D. S. (1996) *J. Am. Chem. Soc. 118*, 3082−3090.
Chakrabartty, A., Schellman, J. A., & Baldwin, R. L. (1991) *Nature 351*, 586−588.
Chakrabartty, A., Kortemme, T., & Baldwin, R. L. (1994) *Prot. Sci. 3*, 843−852.
Chakrabartty, A., Kortemme T., Padmanabhan S., & Baldwin, R. L. (1993) *Biochemistry 32*, 5560−5565.
Chen, Y.-H.; Yang, J. T., & Chau, K. H. (1974) *Biochemistry 13*, 3350−3359.
Conio, G., Patrone, E., & Brighetti, S. (1970) *J. Biol. Chem. 245*, 3335−3340.
Doig, A. J., Chakrabartty, A., Klingler, T. M., & Baldwin, R. L. (1994) *Biochemistry 33*, 3396-3403.
Dyson, H. J., & Wright, P. E. (1993) *Curr. Opin. Struct. Biol. 3*, 60−65.
Fan, P., Bracken, C., & Baum, J. (1993) *Biochemistry 32*, 1573−1582.
Goodman, M., Listowsky, I. (1962) *J. Am. Chem. Soc. 84*, 3770−3771.
Hamada, D., Kuroda, Y., Tanaka, T., & Goto,Y. (1995) *J. Mol. Biol 254*, 737−746.
Hermans, J., Jr., Leach, S. J., & Scheraga, H. A. (1963) *J. Phys. Chem. 85*, 1390−1395.
Jasanoff, A., & Fersht, A. R. (1994) *Biochemistry 33*, 2129−2135.
Johnson, M. L., Correia, J. J., Yphantis, D. A., & Halvorson, H. R. (1981) *Biophys. J. 36*, 575−588.
Lifson, S., & Roig, A. (1961) *J. Chem. Phys. 34*, 1963−1974.
Lotan, N., Bixon, M., & Berger, A. (1967) *Biopolymers 5*, 69−77.
Muñoz, V., & Serrano, L. (1994) *Nature Struct. Biol. 1*, 399−409.

Nelson, J. W., & Kallenbach, N. R. (1986) *Proteins: Struct., Funct., Genet. 1*, 211−217.
Filippi, B., Borin, G., Moretto, V., & Marchiori, F. (1978) *Biopolymers 17*, 2545−2559.
Ramírez-Alvarado, M., Blanco, F. J., & Serrano, L. (1996) *Nature Struct. Biol. 3*, 604−612.
Rohl, C. A. (1996) PhD thesis, Stanford University.
Rohl, C. A., & Baldwin, R. L. (1994) *Biochemistry 33*, 7760−7767.
Rohl, C. A., Chakrabartty, A., & Baldwin, R. L. (1996) *Prot. Sci. 5*, 2623−2637.
Rohl, C. A., Scholtz, J. M., York, E. J., Stewart, J. M., & Baldwin, R. L. (1992) *Biochemistry 31*, 1263−1269.
Scholtz, J. M., Qian, H., York, E. J., Stewart, J. M., & Baldwin, R. L. (1991a) *Biopolymers 31*, 1463−1470.
Scholtz, J. M., Marqusee, S., Baldwin, R. L., York, E., Stewart, J. M., Santoro, M., & Bolen, D. W. (1991b) *Proc. Natl. Acad. Sci. U.S.A. 88*, 2854−2858.
Scholtz, J. M., Barrick, D., York, E. J., Stewart, J. M., & Baldwin, R. L. (1995) *Proc. Natl. Acad. Sci. U.S.A. 92*, 185−189.
Schönbrunner, N., Wey, J., Engels, J., Georg, H., & Kiefhaber, T. (1996) *J. Mol. Biol. 260*, 432−445.
Segawa, S-I., Fukuno, N., Fujiwara, K., & Noda, Y. (1991) *Biopolymers 31*, 497−509.
Shan, S.-O., & Herschlag, D. (1996) *Proc. Natl. Acad. Sci. USA 93*, 14474−14479.
Shin, H.-C., Merutka, G., Waltho, J., Wright, P. E, & Dyson, H. J. (1993a) *Biochemistry 32*, 6348−6355.
Shin, H.-C., Merutka, G., Waltho, J., Tennant, L. L., Dyson, H. J., & Wright, P. E (1993b) *Biochemistry 32*, 6356−6364.
Smith, J. S., & Scholtz, J. M. (1996) *Biochemistry 35*, 7292−7297.
Sönnichsen, F. D., Van Eyk, J. E., Hodges, R. S., & Sykes, B. D. (1992) *Biochemistry 31*, 8790−8798.
Storrs, R. W., Truckses, D., & Wemmer, D. E. (1992) *Biopolymers 32*, 1695−1702.
Wang, J., & Purisima, E. O. (1996) *J. Am. Chem. Soc. 118*, 995−1001.
Waltho, J., Feher, V. A., Merutka, G., Dyson, H. J., & Wright, P. E. (1993) *Biochemistry 32*, 6337−6347.
Yang, A. S., Sharp, K. A., & Honig, B. (1992) *J. Mol. Biol. 227*, 889−900.
Zimm, B. H., & Brag, J. K. (1959) *J. Chem. Phys. 31*, 526−535.
Zimm, B. H., Doty, P., & Iso, K. (1959) *Proc. Natl. Acad. Sci. U.S.A. 45*, 1601−1607.

BI9707133